Physics Letters B 797 (2019) 134900

Contents lists available at ScienceDirect

Physics Letters B

www.elsevier.com/locate/physletb

Cross section of the reaction $^{18}O(p,\gamma)^{19}F$ at astrophysical energies: The 90 keV resonance and the direct capture component

A. Best [d,e,*], F.R. Pantaleo [f,g], A. Boeltzig [a,b,c,1], G. Imbriani [d,e], M. Aliotta [h], J. Balibrea-Correa [d,e], D. Bemmerer [i], C. Broggini [k], C.G. Bruno [h], R. Buompane [e,j], A. Caciolli [l,k], F. Cavanna [m], T. Chillery [h], G.F. Ciani [a,c], P. Corvisiero [n,m], L. Csedreki [c,a], T. Davinson [h], R.J. deBoer [b], R. Depalo [l,k], A. Di Leva [d,e], Z. Elekes [o], F. Ferraro [n,m], E.M. Fiore [f,g], A. Formicola [c], Zs. Fülöp [o], G. Gervino [p,q], A. Guglielmetti [r,s], C. Gustavino [t], Gy. Gyürky [o], M. Junker [c,a], I. Kochanek [c], M. Lugaro [u], P. Marigo [k,l], R. Menegazzo [k], V. Mossa [f,g], V. Paticchio [g], R. Perrino [g,1], D. Piatti [l,k], P. Prati [n,m], L. Schiavulli [f,g], K. Stöckel [i,v], O. Straniero [w,c], F. Strieder [x], T. Szücs [i], M.P. Takács [i,v,2], D. Trezzi [r,s], M. Wiescher [b], S. Zavatarelli [m]

[a] *Gran Sasso Science Institute, Viale F. Crispi 7, 67100 L'Aquila, Italy*
[b] *The Joint Institute for Nuclear Astrophysics, Department of Physics, University of Notre Dame, Notre Dame, IN 46556, USA*
[c] *Istituto Nazionale di Fisica Nucleare, Laboratori Nazionali del Gran Sasso (LNGS), Via G. Acitelli 22, 67100 Assergi, Italy*
[d] *Università degli Studi di Napoli "Federico II", Dipartimento di Fisica "E. Pancini", Via Cintia 21, 80126 Napoli, Italy*
[e] *Istituto Nazionale di Fisica Nucleare, Sezione di Napoli, Via Cintia 21, 80126 Napoli, Italy*
[f] *Università degli Studi di Bari, Dipartimento Interateneo di Fisica, Via G. Amendola 173, 70126 Bari, Italy*
[g] *Istituto Nazionale di Fisica Nucleare, Sezione di Bari, Via E. Orabona 4, 70125 Bari, Italy*
[h] *School of Physics and Astronomy, University of Edinburgh, Peter Guthrie Tait Road, EH9 3FD Edinburgh, United Kingdom*
[i] *Helmholtz-Zentrum Dresden-Rossendorf, Bautzner Landstraße 400, 01328 Dresden, Germany*
[j] *Università degli Studi della Campania "L. Vanvitelli", Dipartimento di Matematica e Fisica, Viale Lincoln 5, 81100 Caserta, Italy*
[k] *Istituto Nazionale di Fisica Nucleare, Sezione di Padova, Via F. Marzolo 8, 35131 Padova, Italy*
[l] *Università degli Studi di Padova, Via F. Marzolo 8, 35131 Padova, Italy*
[m] *Istituto Nazionale di Fisica Nucleare, Sezione di Genova, Via Dodecaneso 33, 16146 Genova, Italy*
[n] *Università degli Studi di Genova, Via Dodecaneso 33, 16146 Genova, Italy*
[o] *Institute for Nuclear Research of the Hungarian Academy of Sciences (MTA Atomki), PO Box 51, 4001 Debrecen, Hungary*
[p] *Università degli Studi di Torino, Via P. Giuria 1, 10125 Torino, Italy*
[q] *Istituto Nazionale di Fisica Nucleare, Sezione di Torino, Via P. Giuria 1, 10125 Torino, Italy*
[r] *Università degli Studi di Milano, Via G. Celoria 16, 20133 Milano, Italy*
[s] *Istituto Nazionale di Fisica Nucleare, Sezione di Milano, Via G. Celoria 16, 20133 Milano, Italy*
[t] *Istituto Nazionale di Fisica Nucleare, Sezione di Roma, Piazzale A. Moro 2, 00185 Roma, Italy*
[u] *Konkoly Observatory, Research Centre for Astronomy and Earth Sciences, Hungarian Academy of Sciences, 1121 Budapest, Hungary*
[v] *Technische Universität Dresden, Institut für Kern- und Teilchenphysik, Zellescher Weg 19, 01069 Dresden, Germany*
[w] *INAF – Osservatorio Astronomico d'Abruzzo, Via Mentore Maggini, 64100 Teramo, Italy*
[x] *Department of Physics, South Dakota School of Mines and Technology, 501E St Joseph Street, Rapid City, SD 57701, USA*

ARTICLE INFO

Article history:
Received 3 July 2019
Received in revised form 26 August 2019
Accepted 27 August 2019
Available online 30 August 2019
Editor: W. Haxton

ABSTRACT

The observation of oxygen isotopes in giant stars sheds light on mixing processes operating in their interiors. Due to the very strong correlation between nuclear burning and mixing processes it is very important to reduce the uncertainty on the cross sections of the nuclear reactions that are involved. In this paper we focus our attention on the reaction $^{18}O(p,\gamma)^{19}F$. While the $^{18}O(p,\alpha)^{15}N$ channel is thought to be dominant, the (p,γ) channel can still be an important component in stellar burning in giants, depending on the low energy cross section. So far only extrapolations from higher-energy

* Corresponding author at: Università degli Studi di Napoli "Federico II", Dipartimento di Fisica "E. Pancini", Via Cintia 21, 80126 Napoli, Italy.
E-mail address: best@na.infn.it (A. Best).

[1] Permanent address: Istituto Nazionale di Fisica Nucleare, Sezione di Lecce, Via Arnesano, 73100 Lecce, Italy.
[2] Current address: Physikalisch-Technische Bundesanstalt, Bundesallee 100, 38116 Braunschweig, Germany.

https://doi.org/10.1016/j.physletb.2019.134900

Keywords:
Experimental nuclear astrophysics
Underground nuclear physics
Hydrogen burning
Stellar evolution

measurements exist and recent estimates vary by orders of magnitude. These large uncertainties call for an experimental reinvestigation of this reaction. We present a direct measurement of the $^{18}O(p,\gamma)^{19}F$ cross section using a high-efficiency 4π BGO summing detector at the Laboratory for Underground Nuclear Astrophysics (LUNA). The reaction cross section has been directly determined for the first time from 140 keV down to 85 keV and the different cross section components have been obtained individually. The previously highly uncertain strength of the 90 keV resonance was found to be 0.53 ± 0.07 neV, three orders of magnitude lower than an indirect estimate based on nuclear properties of the resonant state and a factor of 20 lower than a recently established upper limit, excluding the possibility that the 90 keV resonance can contribute significantly to the stellar reaction rate.

The observation of oxygen isotopes in evolved giant stars provides unique information on various mixing processes operating in stellar interiors, among them those induced by convection, rotation and magnetic fields [1–6]. Oxygen isotopic ratios can be used to determine the efficiency of these mixing processes. For instance, in the innermost portion of the H-rich envelope of a star climbing the red giant branch (RGB) or the asymptotic giant branch (AGB), where the temperature exceeds ~ 20 MK, ^{18}O is efficiently destroyed by proton captures (see figure 5 in [7]). If some instability inducing a mixing process extends down to this region, an increase of the $^{16}O/^{18}O$ ratio should be observed at the stellar surface (see figures 6 and 7 in [7]). The observed ratio is particularly sensitive to the maximum temperature attained by the instability responsible for the mixing. However, the effective application of this chemical probe requires a precise evaluation of the low-energy rates of the two ^{18}O proton-capture channels, i.e., the reactions $^{18}O(p,\alpha)^{15}N$ and $^{18}O(p,\gamma)^{19}F$.

These two reactions are also important in the long-standing debate about the origin of galactic fluorine (see, e.g. [8]). Fluorine enhancements are commonly observed in thermally pulsing AGB stars [9,10], but the corresponding nucleosynthesis scenario is still largely uncertain (see, e.g. [11,12]). The main production channel should be $^{15}N(\alpha,\gamma)^{19}F$, operating in the He-burning region of an AGB star. In this case the main issue is the amount of ^{15}N available for the fluorine production. According to an early suggestion by [13], ^{15}N is produced by the $^{18}O(p,\alpha)^{15}N$ reaction.[3] An alternative path could be the direct production of fluorine in the H-burning zone through the $^{18}O(p,\gamma)^{19}F$ reaction. Current nucleosynthesis models find that this fluorine source is prevented by the competing $^{18}O(p,\alpha)^{15}N$ reaction and that fluorine is instead depleted in the H-burning zone, mainly through the $^{19}F(p,\alpha)^{16}O$ reaction. Since the reaction $^{18}O(p,\alpha)^{15}N$ dominates over the entire energy range of astrophysical interest (the $\frac{(p,\alpha)}{(p,\gamma)}$ rate ratio ranges from ~ 100 to 10000, depending on the temperature) only a strong increase of the (p, γ) channel cross section could change this occurrence.

Motivated by this astrophysical context, we started a deep underground study of the two ^{18}O proton-capture channels. The results of our recent measurement of $^{18}O(p,\alpha)^{15}N$ is discussed in a separate paper [14]. Here we present our study of the $^{18}O(p,\gamma)^{19}F$ channel.

The most important low energy contributions are the direct capture (DC) cross section, the tail of the strong $E_R = 143$ keV[4] and the previously unmeasured $E_R = 90$ keV resonance. The state in ^{19}F corresponding to the latter resonance ($J^\pi = \frac{3}{2}^+$, $E_x = (8084 \pm 3)$ keV) has been studied recently, yielding inconclusive results. Buckner et al. performed a direct measurement of the low energy $^{18}O(p,\gamma)^{19}F$ cross section [15], resulting in both a much lower DC cross section than measured by Wiescher et al. [16] and in an upper limit of the resonance strength of $\omega\gamma < 7.8$ neV, too low to contribute significantly to the cross section. Shortly thereafter Fortune [17] calculated a resonant cross section based on known nuclear properties of the state. Using literature values of the competing (p,α) channel strength and calculated proton widths, this publication arrived at a much higher recommended value for the resonance strength of $\omega\gamma = (0.7 \pm 0.28)$ μeV. In this case, the 90 keV resonance would provide a significant contribution to the total reaction rate for temperatures between 30 and 80 MK. The resulting rate could be up to a factor 100 higher than that currently adopted in stellar and nucleosynthesis models. Major effects are expected in the case of massive AGB stars undergoing Hot Bottom Burning (HBB) at temperature of about 40-50 MK. In this way, a solution for some puzzling astrophysical cases may be obtained. For instance, many SC stars[5] are fluorine rich, and some of them, such as WZ Cas, show the typical features of a moderate HBB, i.e., substantial Li enhancement together with a rather low C isotopic ratio ($^{12}C/^{13}C \sim 4-5$; see [10]). However, the F enrichment appears incompatible with HBB, unless the branching ratio $< ^{18}O(p,\gamma)^{19}F > / < ^{18}O(p,\alpha)^{15}N >$ is substantially larger than usually adopted, as it would be in the case of a strength of the 90 keV resonance close to the value reported by Fortune.

In order to resolve this ambiguity the $^{18}O(p,\gamma)^{19}F$ low energy cross section, covering the energy region of the 143 keV resonance and below, has been directly measured at the Laboratory for Underground Nuclear Astrophysics (LUNA) [19] at the Gran Sasso National Laboratory in Italy. The measurements discussed here were performed with a large segmented bismuth germanate (BGO) detector surrounding the target in an almost 4π geometry (as detailed in [20]). The detector was surrounded on all sides by at least 10 cm of lead, reducing the low-energy background component by about an order of magnitude. The six BGO detector segments were read out and time-tagged individually and coincident sum spectra were constructed offline. This has the effect of summing up gamma-rays that are emitted in a cascade deexcitation of the resonant state to a single signal at the energy Q value (7993.6 keV [21]) plus the c.m. energy (here between 80 and 150 keV) of the reacting particles. A major advantage of this technique is the shifting of the signal out of the low-energy part of the gamma-ray spectrum that is dominated by natural radioactivity in the laboratory environment into the higher energy region where the prevalent background stems from cosmic-ray interactions with the detector. At LUNA this high-energy background component is reduced by over three orders of magnitude with respect to Earth's surface. The BGO campaign was part of

[3] According to this scenario, part of the ^{15}N is produced in the H-burning shell and the rest in the He burning region, when the s-process nucleosynthesis takes place and fresh protons are released by the $^{14}N(n,p)^{13}C$ reaction.

[4] All energies in this letter are given in the center-of-mass reference frame, unless explicitly stated otherwise.

[5] AGB stars with C/O ≈ 1, see [18] and references therein.

a wider-ranging investigation of the $^{18}O(p,\gamma)^{19}F$ reaction, where the higher-energy resonances and direct capture cross section (up to 400 keV) were also measured with a high purity germanium (HPGe) setup that could be inserted in the same lead shield as the one used for the BGO. The HPGe measurements, including a much more detailed determination of the decay branchings of several resonances, will be presented in a forthcoming publication.

The measurements presented in this letter were performed at the solid target station of the LUNA facility, using anodized Ta_2O_5 targets that were produced with water enriched to 99% ^{18}O. Anodization of tantalum is a standard method that is known to produce homogeneous targets that can withstand high proton beam currents for extended periods [22,23]. Targets with thicknesses (in terms of proton energy loss at 100 keV) of approx. 6 keV and 14 keV, respectively, were employed over the experimental campaign. The thinner targets were used for off-resonance measurements and the thicker ones around the region of the 90 keV resonance. Proton beams of up to 200 μA were delivered onto the water-cooled target and changes in target thickness were regularly monitored by repeated measurements of the yield profile of the 143 keV resonance. Targets were exchanged with fresh ones before reaching a decrease by 10% in maximum yield and thickness. A liquid nitrogen cooled copper pipe extended to the face of the target to reduce carbon deposition on the target. A suppression voltage of -300 V was applied to the copper pipe in order to reflect back sputtered electrons from the target during beam bombardment, eliminating a possible systematic overestimation of the beam current.

The efficiency of the BGO detector, when used in summing mode, is not a simple function of the photon energy. Instead, all possible decay paths from the resonant state to the ground state have to be taken into account with the respective energies and branching ratios of the gamma rays involved. For the setup used here this has been done with a Geant4 [24] simulation that includes all known deexcitation paths of the resonant decay. This simulation has been employed successfully for past measurements at LUNA [25,20] and was revalidated during the current campaign using calibrated sources and well-known resonances in $^{27}Al(p,\gamma)^{28}Si$ and $^{14}N(p,\gamma)^{15}O$. In general, an agreement with the calibration data within a few % was found, but it should be stressed that the efficiency and its uncertainty depends on the knowledge of the branchings of the reaction under study. This will be discussed for the specific case of the present measurement below.

The excitation function of the $^{18}O(p,\gamma)^{19}F$ cross section was measured in steps smaller than the target thicknesses between 85 and 150 keV. Total deposited charges ranged from a few millicoulomb at the highest energies to $\sim$ 40 C at 85 keV. Beam-induced background was checked using an inert target produced with natural H_2O. The count rate in the region of interest around 8 MeV was found to be consistent with the natural background (4×10^{-5} s^{-1} or 4 counts per day). A summed spectrum of all runs taken inside the 90 keV resonance region (the sum of the runs done in the energy range between 90 and 96 keV) is displayed in Fig. 1, showing clear signals at the sum energy for both the resonant energy and below.[6]

The data in the full energy range studied here are comprised of three components: the contributions of the 143 and 90 keV resonances and the direct capture component. The contribution from tails of higher-energy resonances (the closest significantly strong one being at 316 keV) was calculated to be negligible. In order to disentangle the three components from each other the data were fit using an incoherent sum of two Breit-Wigner resonant shapes and a constant "S factor" modeling the direct capture (DC) cross section. The S factor is related to the cross section σ through $\sigma(E) = \frac{1}{E} S(E) e^{-2\pi\eta}$, with the Sommerfeld parameter $\eta = \sqrt{\frac{\mu}{2E}} Z_0 Z_1 e^2$. The $Z_{0,1}e$ are the charges of the reaction partners and μ is the reduced mass.

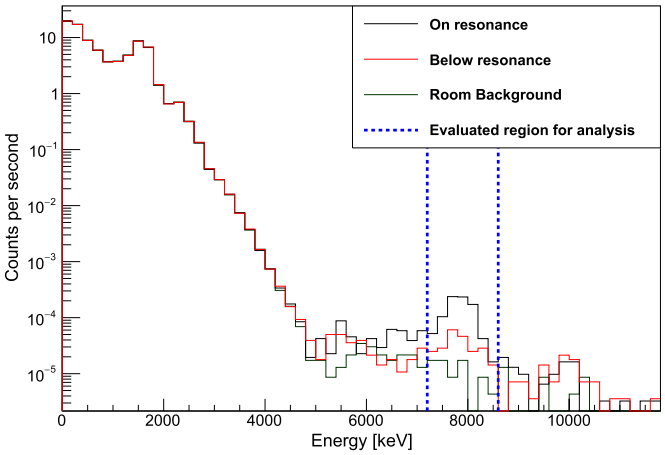

Fig. 1. BGO sum spectra in the on-resonance energy region (black), below the 90 keV resonance (red) and a room background spectrum (green). The two vertical lines delimit the region of interest to calculate the experimental yields.

The strong resonance with E_r = 143 keV can be described using the standard single-level Breit-Wigner formula

$$\sigma_{BW}(E) = \frac{\lambda^2}{4\pi} \frac{2J+1}{(2j_0+1)(2j_1+1)} \frac{\Gamma_p(E)\Gamma_\gamma(E)}{(E_r-E)^2 + \Gamma(E)^2/4} \,. \qquad (1)$$

J, j_0 and j_1 are the spins of the resonant compound state and of the two reaction partners, respectively. The statistical factor involving the different spins is commonly abbreviated as $\omega = \frac{2J+1}{(2j_0+1)(2j_1+1)}$. λ is the de Broglie wavelength and $\Gamma_{p,\gamma}$ are the channel widths (in this case proton and γ) and Γ is the total width of the resonance. The 143 keV resonance is also observed in the (p,α) channel with an α width of 123 eV [26] that completely dominates the total width of the state. It is important to note that the widths are energy dependent and are functions of the Coulomb penetration factors for charged particles and of the multipolarity in the case of photons.

Finally, due to its relative weakness, the 90 keV resonance has been modeled using a simplified Breit-Wigner description with constant widths and introducing the resonance strength $\omega\gamma = \omega\frac{\Gamma_p\Gamma_\gamma}{\Gamma}$. In this case the cross section becomes

$$\sigma_{BW}(E) = \frac{\lambda^2}{4\pi} \omega\gamma \frac{\Gamma}{(E_r-E)^2 + \Gamma^2/4} \,. \qquad (2)$$

The relationship between cross section and measured yield Y is

$$Y(E) = \int_{E-\Delta E}^{E} \eta \frac{\sigma(E)}{\epsilon(E)} dE \,, \qquad (3)$$

[6] The spectra are normalized by measurement time to allow comparison with the room background. For both in-beam measurements similar currents were used, so the ratio of the two spectra approximately represents the yield ratio. The total number of counts in the region of interest for the off-resonance data is 85, of which 21 are expected background counts.

where ϵ is the effective stopping power of the target material[7] and the integration range is determined by the target thickness in terms of the energy loss of the projectile while traversing the target; η is the detection efficiency of the setup. Also here only c.m. values are used in the calculation. When extracting the cross sections of the above mentioned three components one has to assume that each of the two resonant states and the DC part have different γ-ray branchings, and as the detection efficiency of the BGO is a function of the branchings each component contributes to the yield weighted with its efficiency η_i.

$$Y(E) = \int_{E-\Delta E}^{E} \frac{\eta_1 \sigma_{BW_1}(E) + \eta_2 \sigma_{BW_2}(E) + \eta_3 \sigma_{DC}(E)}{\epsilon(E)} dE \qquad (4)$$

Only the branchings of the 143 keV resonance are well known and could be directly used for the efficiency simulation. There is no branching information in the literature on the 90 keV resonance, and only higher-energy direct capture branchings are available [16]. For the low energy resonance we adopted the methodology of Buckner et al.: we calculated efficiencies for the detection of the cascade decay of all states in ^{19}F with known branching ratios, restricting the selection to states with $E_x > 5500$ keV and $J < \frac{9}{2}$. The resulting efficiency distribution was then used for the analysis. The efficiency at $E_x = 8083$ keV, corresponding to the 90 keV resonance was determined by a linear fit through the data. The maximum deviation between simulation points and the fit (evaluated at the resonance state energy) was adopted as the uncertainty of this efficiency determination, resulting in an efficiency of $(59 \pm 7)\%$. The efficiency for the DC component was calculated to be $(49 \pm 5)\%$ using the Wiescher et al. branchings and assuming a conservative uncertainty of 10%.

To calculate the cross sections from the experimental data a least-squares fit was performed in which parameters influencing the different cross section components were allowed to vary freely and the numerically integrated yield was compared to the experimental one. The varied parameters were the $\omega\gamma$ of the low-energy resonance, a scaling factor in the case of the 143 keV resonance and a constant S factor to describe the DC component. The latter choice can be justified by the rather low range in energy between the lowest and highest data point and the fact that the S factor determined over a much larger energy range in the work of Wiescher et al. [16] is not strongly energy dependent. The resonance energy of the low-energy state was set to 90.6 keV and its total width to 121 ± 12 eV [14]. Results of the fit are shown in Fig. 2. The reduced chi-square is 1.22.

The uncertainties in the minimization results were calculated as follows. The low energy resonance width was fixed to random values sampled from a Gaussian distribution with the mean value and FWHM given above and for each value a large number of fits were performed, where the experimental yield data were allowed to vary according to their individual statistical uncertainties, again sampled from a Gaussian distribution. This sampling was repeated many times. The best value for each cross section component was determined as the mean value of the resulting distribution while the corresponding uncertainty was adopted from the average distance between mean value and the 16th and 84th quantiles of this distribution.

The results and a comparison with the literature are shown in Table 1. The following factors were included in the systematic uncertainty: charge integration 3% and 5% from the literature stopping power. 3% were assigned to take into account stoichiometry changes due to target degradation, and 5% to the thickness determination of the used targets. The latter two were included in the individual data points and underwent the Monte Carlo procedure described above. The efficiency for the detection of the DC component was assigned a systematic uncertainty of 10%; due to the much better known branchings of the 143 keV resonance we assigned 5% of uncertainty to its detection efficiency. The strength of the 143 keV resonance is in very good agreement with the literature; the best-fit value of the resonance energy is 143.3 (±

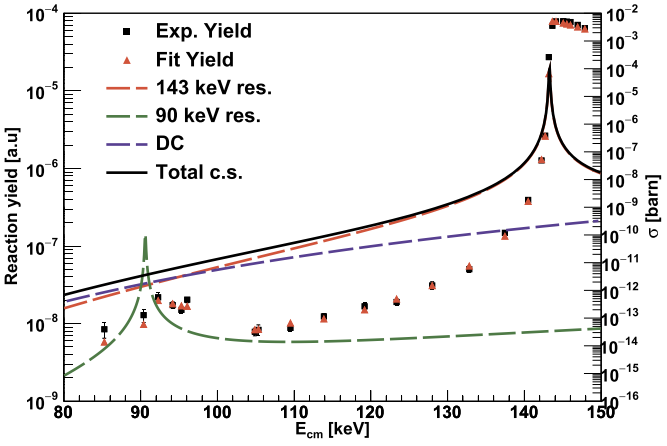

(a)

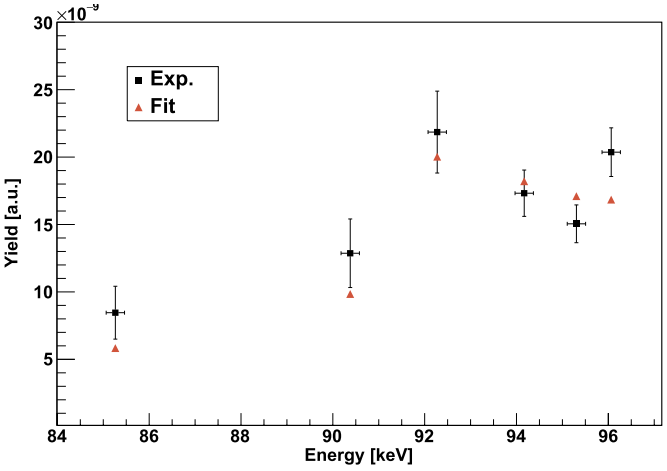

(b)

Fig. 2. (a) Experimental yield and fitted cross section of $^{18}O(p,\gamma)^{19}F$. The total cross section and the direct and resonant components are shown as lines. The left axis refers to the yield points, the right one to the cross sections (lines). Displayed in the inset is a zoom into the low energy resonance region. (b) Experimental data vs. fit results in the low-energy region.

Table 1
Quantities determining the three components of the low-energy $^{18}O(p,\gamma)^{19}F$ cross section.

Fit parameter	Value	Literature
$\omega\gamma$(143 keV) [meV]	0.88 ± 0.07 (sys.)	0.92 ± 0.06 [28] 1.0 ± 0.1 [16]
$\omega\gamma$(90 keV) [neV]	$0.53 \pm {}^{0.07\ stat.}_{0.07\ sys.}$	< 8 [15] $0.7^{+0.56}_{-0.38} \cdot 10^3$ [17]
S_0(DC) [keV b]	$23.0 \pm {}^{2.7\ stat.}_{2.7\ sys.}$	7.06 [15] 15.7 [16]

[7] SRIM-2013 [27] was used to calculate the stopping power of the Ta_2O_5 targets. At 90.4 keV $\epsilon(Ta_2^{18}O_5) = 2.81 \cdot 10^{-14}$ eV cm^2. The stopping power has been scaled by the factor $m_{target}/(m_{target}+m_{beam})$.

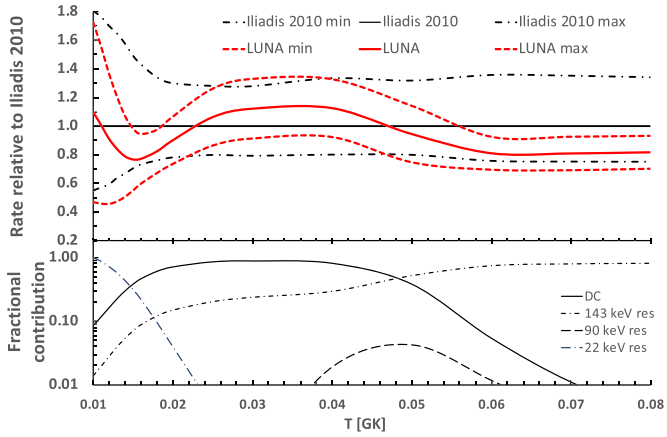

Fig. 3. Top: Reaction rate relative to Iliadis et al. [30]. Bottom: fractional contributions of the individual cross section components to the total rate.

0.3) keV. Our direct measurement of the strength of the 90 keV resonance is in agreement with the Buckner et al. upper limit, which, being much lower than the Fortune calculation [17], leads to a negligible astrophysical importance. The DC S factor was determined directly for the first time at very low energy. We find its value to be 23.0 keV b (corresponding to a DC cross section at 99.4 keV of 5.2 μb), somewhat higher than the Wiescher et al. extrapolation and much higher than the three sigma upper limit given by Buckner et al. It is not entirely clear if or how in the latter work the tail of the 143 keV resonance was considered in the determination of the upper limit, but it does not appear a likely candidate to resolve the difference. The experimental cross sections presented here were corrected for electron screening effects [25,29].[8]

The top part of Fig. 3 shows the low-temperature reaction rate using the experimental results of the present work relative to the literature rate from [30].[9] Our rate, while overall being a bit lower, still agrees very well with the literature. The rate in the higher-temperature range is dominated by the 140 keV resonance. It is lower than the literature due to both the reduced strength and the slightly higher energy than the one used in [30]. The contribution of the individual components to the total rate is shown in the bottom part of Fig. 3. The main result is that the 90 keV resonance only contributes at most a few percent to the reaction rate and does not play an important astrophysical role.

In summary we were able to perform a direct measurement of the very low energy cross section of the reaction $^{18}O(p,\gamma)^{19}F$. We can exclude a very strong 90 keV resonance, in agreement with [15], ruling out the possibility that it plays a role in the ^{19}F production in AGB stars, and through the determination of the S factor to below 90 keV, where it is the dominant contributor to the total cross section, we are able to confirm the present picture of the astrophysical role of $^{18}O(p,\gamma)^{19}F$, improving the uncertainty at the lowest energies. The low energy resonance and the strength of the DC component are now known with precisions of approx. 20% and 15%, respectively. We have confirmed that the stellar reaction rate for the conditions present in low mass AGB stars is dominated by the DC component and the 143 keV resonance, as the low-energy resonance is too weak to play a role. Thanks to our new results it will be possible to perform more firm nucleosynthesis calculations regarding the origin of oxygen polluters in the universe and mixing processes in RGB and AGB stars.

[8] A screening potential of 0.66 keV was used for the calculation. Resulting corrections range between ∼ 10% and 4%, depending on the energy.

[9] This reference was chosen because it appears that the 22 keV resonance was not included to produce the rate table in [15], leading to a much lower rate at the lowest temperatures.

Acknowledgements

This work was supported by the INFN. The authors acknowledge the support at the Gran Sasso National Laboratory, and would like to thank D. Ciccotti and L. Roscilli as well as to the mechanical workshops of the INFN sections of LNGS and Naples. Following authors acknowledge funding from several institutions and grants: Z.E., Z.F., G.Gy.: NKFIH K120666; C.Bru., M.A., T.D.: STFC UK; D.B., M.T., T.S., K.S.: DFG (BE 4100/4-1), Helmholtz Association (NAVI and ERC-RA-0016), COST (ChETEC, CA16117); A.B., J.B., A.D.L., G.I: the University of Naples/Compagnia di San Paolo grant STAR.

References

[1] D.S.P. Dearborn, Phys. Rep. 210 (1992) 367.
[2] A.I. Boothroyd, I.-J. Sackmann, G.J. Wasserburg, Astrophys. J. Lett. 430 (1994) L77.
[3] K.M. Nollett, M. Busso, G.J. Wasserburg, Astrophys. J. 582 (2003) 1036, arXiv:astro-ph/0211271.
[4] P.P. Eggleton, D.S.P. Dearborn, J.C. Lattanzio, Astrophys. J. 677 (2008) 581–592, arXiv:0706.2710.
[5] C. Charbonnel, N. Lagarde, Astron. Astrophys. 522 (2010) A10, arXiv:1006.5359.
[6] S. Palmerini, M. La Cognata, S. Cristallo, M. Busso, Astrophys. J. 729 (2011) 3, arXiv:1011.3948.
[7] O. Straniero, C.G. Bruno, M. Aliotta, A. Best, A. Boeltzig, D. Bemmerer, C. Broggini, A. Caciolli, F. Cavanna, G.F. Ciani, et al., Astron. Astrophys. 598 (2017) A128, arXiv:1611.00632.
[8] H. Jönsson, N. Ryde, G.M. Harper, M.J. Richter, K.H. Hinkle, Astrophys. J. Lett. 789 (2014) L41, arXiv:1406.4876.
[9] A. Jorissen, V.V. Smith, D.L. Lambert, Astron. Astrophys. 261 (1992) 164.
[10] C. Abia, K. Cunha, S. Cristallo, P. de Laverny, I. Domínguez, K. Eriksson, L. Gialanella, K. Hinkle, G. Imbriani, A. Recio-Blanco, et al., Astrophys. J. Lett. 715 (2010) L94.
[11] M. Lugaro, C. Ugalde, A.I. Karakas, J. Görres, M. Wiescher, J.C. Lattanzio, R.C. Cannon, Astrophys. J. 615 (2004) 934, arXiv:astro-ph/0407551.
[12] S. Cristallo, A. Di Leva, G. Imbriani, L. Piersanti, C. Abia, L. Gialanella, O. Straniero, Astron. Astrophys. 570 (2014) A46, arXiv:1408.2986.
[13] M. Forestini, S. Goriely, A. Jorissen, M. Arnould, Astron. Astrophys. 261 (1992) 157.
[14] C. Bruno, M. Aliotta, P. Descouvemont, A. Best, T. Davinson, D. Bemmerer, A. Boeltzig, C. Broggini, A. Caciolli, F. Cavanna, et al., Phys. Lett. B (ISSN 0370-2693) 790 (2019) 237, http://www.sciencedirect.com/science/article/pii/S0370269319300334.
[15] M.Q. Buckner, C. Iliadis, J.M. Cesaratto, C. Howard, T.B. Clegg, A.E. Champagne, S. Daigle, Phys. Rev. C 86 (2012) 065804.
[16] M. Wiescher, H.W. Becker, J. Görres, K.-U. Kettner, H.P. Trautvetter, W.E. Kieser, C. Rolfs, R.E. Azuma, K.P. Jackson, J.W. Hammer, Nucl. Phys. A 349 (1980) 165.
[17] H.T. Fortune, Phys. Rev. C 88 (2013) 015801.
[18] C. Abia, I. Domínguez, R. Gallino, M. Busso, O. Straniero, P. de Laverny, G. Wallerstein, Publ. Astron. Soc. Aust. 20 (2003) 314.
[19] H. Costantini, A. Formicola, G. Imbriani, M. Junker, C. Rolfs, F. Strieder, Rep. Prog. Phys. 72 (2009) 086301.
[20] A. Boeltzig, A. Best, G. Imbriani, M. Junker, M. Aliotta, D. Bemmerer, C. Broggini, C.G. Bruno, R. Buompane, A. Caciolli, et al., J. Phys. G, Nucl. Part. Phys. 45 (2018) 025203, http://stacks.iop.org/0954-3899/45/i=2/a=025203.
[21] M. Wang, G. Audi, F. Kondev, W. Huang, S. Naimi, X. Xu, Chin. Phys. C 41 (2017) 030003.
[22] D. Vermilyea, Acta Metall. 1 (1953) 282.
[23] A. Caciolli, D.A. Scott, A. Di Leva, A. Formicola, M. Aliotta, M. Anders, A. Bellini, D. Bemmerer, C. Broggini, M. Campeggio, et al., Eur. Phys. J. A 48 (2012) 144.
[24] S. Agostinelli, et al., Nucl. Instrum. Methods A 506 (2003) 250.
[25] F. Strieder, B. Limata, A. Formicola, G. Imbriani, M. Junker, D. Bemmerer, A. Best, C. Broggini, A. Caciolli, P. Corvisiero, et al., Phys. Lett. B (ISSN 0370-2693) 707 (2012) 60, http://www.sciencedirect.com/science/article/pii/S0370269311014869.

[26] C. Iliadis, R. Longland, A. Champagne, A. Coc, in: The 2010 Evaluation of Monte Carlo based Thermonuclear Reaction Rates, Nucl. Phys. A (ISSN 0375-9474) 841 (2010) 251, http://www.sciencedirect.com/science/article/pii/S0375947410004203.
[27] J. Ziegler, Nucl. Instrum. Methods B 219 (2004) 1027, software version SRIM-2010, http://www.srim.org.
[28] R.B. Vogelaar, T.R. Wang, S.E. Kellogg, R.W. Kavanagh, Phys. Rev. C 42 (1990) 753, https://link.aps.org/doi/10.1103/PhysRevC.42.753.
[29] H.J. Assenbaum, K. Langanke, C. Rolfs, Z. Phys. A (ISSN 0939-7922) 327 (1987) 461, https://doi.org/10.1007/BF01289572.
[30] C. Iliadis, R. Longland, A. Champagne, A. Coc, R. Fitzgerald, in: The 2010 Evaluation of Monte Carlo based Thermonuclear Reaction Rates, Nucl. Phys. A (ISSN 0375-9474) 841 (2010) 31, http://www.sciencedirect.com/science/article/pii/S0375947410004197.